ISSN 1063-7729, Astronomy Reports, 2013, Vol. 57, No. 3, pp. 195–211. © Pleiades Publishing, Ltd., 2013.
Original Russian Text © A.I. Zakharov, A.V. Mironov, M.E. Prokhorov, A.V. Biryukov, O.Yu. Stekol'shchikov, M.S. Tuchin, 2013, published in Astronomicheskii Zhurnal, 2013, Vol. 90, No. 3, pp. 223–241.

The LYRA-B Space Experiment: Goals and Principles for Its Realization

A. I. Zakharov, A. V. Mironov, M. E. Prokhorov*, A. V. Biryukov, O. Yu. Stekol'shchikov, and M. S. Tuchin

Sternberg Astronomical Institute, Lomonosov Moscow State University, Uiversitetskii pr. 13, Moscow, 119991 Russia

Received June 14, 2012; in final form, July 12, 2012

Abstract—We describe goals and principles for the realization the Lyra-B space experiment onboard the International Space Station, which is currently being prepared at the Sternberg Astronomical Institute. The main goal of the experiment is to carry out a high-accuracy, multicolor all-sky survey of stars down to 16^m–17^m. The detailed structure of the expected observational data, their possible scientific use, and a number of technical problems are discussed.

DOI: 10.1134/S1063772913030062

1. INTRODUCTION

Compiling catalogs of stars and other celestial objects is a classical task of astronomy. Such catalogs are used by astronomers to extract basic information for statistical studies and to select objects for detailed investigation.

The first really large catalogs were created during the last decade of the 20th century, through scanning and digitizing plates of the Palomar Sky Survey [1–3] and some other photographic surveys. The "Guide Star Catalog" (GSC) and USNO catalogs were compiled in this way.

Early versions of the GSC catalog [4–8] contain about 19 million objects, of which some 15 million are classified as stars brighter than 16^m. The photographic magnitudes of stars in the GSC 1.1 and GSC 1.2 releases of the catalog are given in only one spectral band. The latest release, GSC 2.3.2 [9], contains more than 950 million objects down to about 22^m, at least half of which are stars; photographic magnitudes are presented in four spectral bands: two blue bands and two bands corresponding to the red and near-infrared. The magnitudes in the GSC catalogs for stars brighter than approximately 12^m, whose images are saturated on the photographic plates, were taken from the Tycho-2 catalog [10] or other catalogs of photoelectric magnitudes in the Johnson B and V bands.

The USNO-A2.0 and USNO-B1.0 catalogs [11, 12] contain about 500 million and one billion objects, respectively. Photographic magnitudes in the USNO-A2.0 catalog are presented for two (blue and red) bands; those in the USNO-B1.0 catalog are presented for five spectral bands (two blue, two red, and one infrared).

The magnitudes in the GSC and USNO catalogs are not very accurate. The random uncertainties within a single photographic plate are 0.1^m–0.2^m. The systematic uncertainties between magnitudes estimated using different plates are much higher, and can reach 0.5^m or more; it is they that determine the uncertainties of the catalog as a whole.

Later, catalogs comparable in volume to the GSC and USNO catalogs were created based on direct photoelectric measurements of light fluxes from stars—the Two Micron All Sky Survey (2MASS) [13] and Sloan Digital Sky Survey (SDSS) [14]. These are multicolor catalogs with deep limiting magnitudes (Table 1). However, they were not created using the procedures required for high photometric accuracy (such as accurate correction for atmospheric extinction), and, while their random errors are at an acceptable level, their systematic uncertainties are too large for the data to be used as magnitude standards for accurate photometry [17].

Currently, the most accurate photometric catalogs are part of the Hipparcos catalog [15] and the Tian Shan $WBVR$ catalog of the Sternberg Astronomical Institute (SAI) [16]. The first of these contains about 118 000 stars spread over the entire sky measured in the one Hp band, approximately to 12^m. About 75% of the catalog's stars brighter than 9.5^m have Hp-magnitude uncertainties no greater than 0.003^m. The second catalog contains about 13 600 stars of the Northern sky ($\delta > -15°$) down to 7.2^m, measured in four bands. The internal uncertainties of these

*E-mail: mike.prokhorov@gmail.com

Table 1. Characteristics of the best-known photometric stellar catalogs

Catalog	Magnitudes	Spectral bands	Number of objects	Uncertainty	Sky coverage
Hipparcos [15]	0–9	1 (Hp)	~118 000	0.001^m	100%
Tycho-2 [10]	0–12	2 (B_T, V_T)	2.5 mln	0.01^m	100%
Tian Shan [16]	0–7.2	4 (W, B, V, R)	~12 000	0.002^m	$\delta > -15°$
GSC 1.2 [8]	0–16	2 (B_T, V_T)	15 mln	$>0.1^m$	100%
GSC 2.3 [9]	12–22	3 (B_T, V_T)	950 mln	$>0.1^m$	100%
USNO-A2.0 [11]	10–21	3 (B_T, V_T)	500 mln	$>0.1^m$	100%
USNO-B1.0 [12]	10–21	3 (B_T, V_T)	1 bln	$>0.1^m$	100%
2MASS [13]	5–16	3 (J, H, K)	470 mln	0.04^m	100%
SDSS(DR8) [14]	16–22.5	5 (u, g, r, i, z)	260 mln	0.04^m	14 500 sq. deg

catalogs are of order $0.001–0.003^m$; the mutual uncertainty of the catalogs estimated from observations of non-variable stars does not exceed 0.003^m [18, 19].

Wide spectral coverage is desirable for modern photometric catalogs. Various sky surveys in the UV and IR have recently been carried out, are being carried out now, or are planned [13, 20–23]. The paradox of the current situation is that there is a lack of simultaneous measurements in different parts of the optical range, making it impossible to relate these surveys to each other, or to find reliable color indices for variable and unique objects.

We list the requirements for modern photometric catalogs below:

- a large number of photometric bands (four to five in the visible; coverage of the IR and UV is also desirable);
- a moderately deep ($16^m–17^m$) or very deep ($>20^m$) limiting magnitude;
- low random and systematic uncertainties (of the order of 0.01^m at the magnitude limit and within 0.001^m for objects $4^m–5^m$ brighter than the limit);
- coverage of the entire celestial sphere.

Table 1 shows to what extent the main existing catalogs satisfy these requirements. It is apparent from the table that there are currently no *high-accuracy milticolor photoelectric* star catalogs that satisfy all these conditions.

According to the results presented in [24, 25], the statistical errors for observations of bright stars due to atmospheric fluctuations decrease much more slowly than other kinds of errors. Therefore, the time needed to perform a deep, accurate photometric survey from the ground becomes unacceptably long. This means that such surveys must be performed from space. Ground-based observations also do not enable measurements in the UV and in part of the IR.

The sky survey to be performed during the Lyra-B space experiment solves these problems; the catalog to be compiled after the completion of the experiment will satisfy all of the above requirements.

Section 2 describes the main goals of the Lyra-B experiment. Section 3 deals with the key directions of astronomical research that will become possible thanks to the results of this experiment. Section 4 is concerned with the principles of the sky survey. Section 5 discusses why the International Space Station (ISS) was chosen as the site of the Lyra-B experiment. The results expected from the survey and the structure of the scientific data to be obtained are considered in Section 6. Finally, Section 7 presents our conclusions.

2. THE GOALS OF THE "LYRA-B" SPACE EXPERIMENT

The aim of the experiment is to carry out a high-accuracy multicolor photometric survey of all celestial objects between 3^m and 16^m. During the experiment (which will last from 3.5 to 5 yrs), it is planned to perform multiple photometric measurements of objects in 10 spectral bands, ranging approximately from 200 to 1000 nm. The experiment should result in the following catalogs:

- a catalog of non-variable stars brighter than 12^m, with uncertainties not exceeding 0.1–0.2% ($0.001^m–0.002^m$); special precautions will be taken to accurately measure the brightest stars to 3^m, also in the B and V bands;

- a catalog (atlas) of non-variable stars brighter than 16^m; uncertainties not exceeding 1% (0.01^m) should be achieved in the B and V bands;
- a catalog of variable stars brighter than 16^m;
- a multicolor photometric catalog of asteroids brighter than 14^m;
- a catalog of stellar positions, with uncertainties of about 100–200 microarcseconds for bright stars and 1 milliarcsecond (mas) for other stars;
- a multicolor catalog of extended objects with high surface brightness;
- an atlas of the background sky in all spectral bands of the survey.

Most stars to be detected in the survey are red. The maximum of their light is in the long-wavelength part of the visible or the near-infrared. The 2MASS infrared survey [13] suggests that data for at least 100 million stars will be recorded in the Lyra-B experiment. A more careful estimate shows that about 350 million stars will have their V magnitudes measured with uncertainties within 0.01^m [26].

The sense in which the survey has high accuracy is that, in the bands where the stellar flux is highest, all *non-variable stars* brighter than 12^m will be measured with final uncertainties not exceeding 0.001^m, and fainter objects with uncertainties not exceeding 0.01^m–0.02^m. Special measures will be taken in order to obtain high-accuracy magnitudes for the brightest stars, up to 3^m.

The main features of the Lyra-B survey are:

- quasi-simultaneous (within 15–20 s) multicolor photometric measurements of objects over a wide spectral range;
- high accuracy of photometric measurements, achieved by performing multiple measurements of objects at time intervals much shorter than the time scales for variations of the instrumental parameters;
- special measures to be taken for accurate brightness determination for stars between 3^m and 16^m–17^m, making it possible to overcome limitations imposed by the light detector's limited dynamic range (see Section 4.4.6).

Much information that is important for various branches of astronomy can be obtained from the experiment data. The most obvious areas of application of the data are considered in Section 3.

Another significant characteristic of the Lyra-B space experiment is that it will be performed onboard the ISS [27]. The reasons for this choice of site are described below, in Section 5. Limitations due to the location of the scientific equipment onboard the ISS determine many of the experiment's characteristics and the technical solutions applied in its set of scientific equipment.

3. SCIENTIFIC GOALS OF THE "LYRA-B" SPACE EXPERIMENT

Variouse scientific results can be expected from the data to be obtained in the Lyra-B experiment, and a serious consideration of this topic lies far beyond the scope of this paper. We present a brief list of the main, most obvious research directions below. Note that the structure of the data provided by the experiment, described in Section 6, will significantly influence possibilities for studies of various celestial objects.

3.1. Creation of the High-Accuracy, Multicolor, Photometric Star Catalog and Related Issues

The catalog we expect to create in the Lyra-B experiment should solve the problem of consistency of magnitudes for stars of different spectral types at wavelengths between 200 nm and 1000 nm.

As was noted above, the Lyra-B experiment will measure the magnitudes of all celestial objects down to 12^m with uncertainties below 0.001^m. Special measures will be taken to have the same small uncertainties for the brightest stars, up to 3^m. A considerably larger number of fainter objects (down to approximately 16^m) will be measured with uncertainties within 0.01^m. Such measurements are not very valuable photometrically; however, they will be accompanied by coordinate determinations with accuracy better than $0.1''$, so that this data set will form a multicolor digital atlas of celestial objects that can form a basis for further multifaceted astronomical studies.

These multicolor measurements will make it possible to develop a very reliable, uniform system of photometric standard stars down to 12^m–14^m, with uncertainties of 0.001^m–0.002^m, over a wide spectral range and covering the entire sky. The mean density of these standard stars will be at least 25 stars/deg^2. There is no doubt of the need to create such a system, due to the wide use of CCD detectors for multicolor photometry: such measurements cannot be related

to the much brighter photometric standards that are currently known. The new system of standard star will also enable photometric calibration of various UV and IR photometric systems and correction for systematic errors related to the time instability of the reaction curves [28].

Based on the catalog of standard stars and the multicolor digital sky atlas, it will be possible to develop techniques for wide-field and sub-pixel ground-based photometry with moderate accuracy (0.01^m–0.05^m). Such techniques can be used to carry out large numbers of systematic observations of different types of objects (variable stars, asteroids, artificial Earth satellites, etc.) with wide-field instruments.

Images of all objects whose signals in a panchromatic band exceed the established threshold will be recorded in all the photometric bands and sent to the Earth. These images will cover about 1% of the celestial sphere. However, the signals detected between bright objects are also of interest. Their level is low, and pixel-to-pixel recording would bring them below the readout noise. Such signals will be summed without readout in order to estimate the background from unresolved sources. These recordings can be used to evaluate the background level or to plot a map of the background, as well as to search for sources that are below the limit of the main, systematic survey. One of the tasks to be addressed is to plot a multicolor map of the zodiacal light and gegenschein, to determine the location and physical properties of the dust grains giving rise to this diffuse light.

The reaction curves of the equipment installed at the ISS will be subject to changes due to contamination by components of the microatmosphere, the influence of cosmic rays, and aging of the materials. However, the large numbers of measurements of non-variable stars that will be carried out in the Lyra-B experiment and the regular application of special calibration procedures will enable identification of variations in the reaction curves and the reduction of systematic errors in the data.

The reliable detection and subsequent elimination of systematic errors requires specially planned, coordinated ground-based observations. It is also desirable to consider possibilities for returning optical filters and CCD chips to the Earth after the end of the Lyra-B experiment, for subsequent metrological and materials-science investigations. This will enable a considerable increase in the reliability of the photometric measurements of objects acquired during the experiment.

3.2. Photometric Studies of the Surfaces of Minor Solar-System Bodies

It is unlikely that the Lyra-B experiment will discover many new asteroids or comets, since the telescope aperture is too small to detect faint objects and the telescope's field of view is much narrower than those of instruments used in programs aimed at searches for asteroids and comets. The Lyra-B experiment will detect only fairly bright objects in the main asteroid belt or even more nearby objects. The orbits of most of these are already known. On the other hand, every observed asteroid will enter the telescope's field of view 100 times during the experiment, on average. With an uncertainty for a single set of coordinate measurements from $0.01''$ to $0.1''$, this will enable a significant improvement of the orbital parameters. However, given the time structure of the observations (see Section 6), a special adaptation of algorithms used for the determination and improvement of orbits may be needed.

The most interesting data on asteroids will probably be multicolor photometry, which will provide information about the physical properties of the objects' surfaces and refine their classification. Multiple observations of asteroids at short time intervals (see Section 6) may make it possible to draw conclusions about their axial rotation.

3.3. Galactic Studies

The compilation of a catalog of high-precision flux measurements for stars in several spectral bands opens wide possibilities for Galactic astronomy and astrophysics, which is especially important given prospects for obtaining accurate coordinates and parallaxes for large numbers of objects in the foreseeable future [29]. Together with highly accurate photometric measurements, these data can be used to study fine statistical regularities in the Galactic structure, the distribution of absorbing matter in the Galaxy, and the physical characteristics (luminosities, chemical composition, surface gravities, rotation rates, etc.) of millions of Galactic stars. These data can be used to improve stellar evolutionary tracks, study their features in more detail, etc. It is beyond the scope of this paper to formulate and list the many problems that can be addressed with such statistical material.

3.4. Multicolor Surface Photometry for Extended Objects

In the case of galaxies and nebulae, the typical surface brightness of extended objects is 18^m arriving from a square arcsecond or less. Such brightnesses are close to the detection limit of the Lyra-B experiment (see Section 6). To detect such objects, it will be

necessary to apply a binning procedure; i.e., to sum signals from several pixels, resulting in decreased noise. Areas occupied by extended objects and the detection modes used to image them will be listed in a special catalog of such objects.

Regions of the celestial sphere containing extended objects will be observed in all the spectral bands each time such objects enter the scanning strip. This scanning will be performed from different directions, with arbitrary pixel shifts compared to images obtained earlier. The number of measurements of extended objects will be the same as for stars: on average, 100 times during the five years of the experiment. All recorded scans will be used to derive unified, multicolor, photometric maps of their surface brightnesses.

3.5. Determination of Distances to Stars from Interstellar Extinction in the UV

The UV bands of the Lyra-B photometric system were selected so that the middle one (218 nm) coincides with an interstellar absorption band, while the others (195 and 270 nm) lie at shorter and longer wavelengths relative to this band. Measurements in these bands, or at least the two longer-wavelength ones, enable estimation of the interstellar extinction. Comparing the observed extinction for a star with a three-dimensional interstellar-extinction map based on the spatial distribution of interstellar hydrogen [30] can yield rather accurate estimates of the distances to the star.

UV fluxes sufficient for such measurements are emitted by stars of spectral type A or earlier; i.e., this method can be used to estimate the distances to several million stars.

3.6. Discoveries of and Studies of Variable Stars

In the first year of the experiment, each object will be measured, on average, 20 times. The number of measurements is higher near the celestial poles, where it can reach 1000 measurements per year (depending on the scanning mode used for circumpolar regions). Such observations can be used to detect new variable stars (so-called "suspected variable stars" in the terminology of [31][1]) and to study them with data of moderate quality (the number of observations and thereby quality of the data will be higher for circumpolar regions). If at least 1% of stars are variable, the Lyra-B experiment will make it possible to detect more than 1 000 000 variable-star candidates, far more than the number of currently known variable stars.[2] Statistical studies of variable stars discovered in the course of the Lyra-B space experiment will make it possible to find and/or refine the following:

- the distribution of variable stars according to type;
- the spatial distributions of various types of variables and their relationship to the Galactic structure;
- the statistical parallaxes for various types of variable stars and their space density distribution in the Galaxy.

Discoveries of new types of variable stars and refinement of current classifications are also possible.

3.7. Detection of Unresolved Double Stars based on Multicolor Photometry

One way to find binary stars is to identify two components in a star's spectrum that correspond to stars with different surface temperatures.

If the components' temperatures differ only insignificantly and there are no eclipses, it is virtually impossible to distinguish such a binary star from a single stars photometrically. It is easy to identify binary systems with a cool star and a hot star that is smaller in size. In this case, the spectral peak for the hot star will be observed in the Wien range of the cool star, as excess radiation above that from the cool star, even if the hot star has a lower luminosity.

It is nearly impossible to detect binarity in the opposite situation, when the cool star is simultaneously the smaller one. The case of stars with different temperatures but almost the same sizes is also difficult. In this case, the light from the cool star is fainter than the light from the hot star at all wavelengths, but it is possible to notice distortions due to the presence of the cool component in the Rayleigh–Jeans region of the hot star's spectrum. This situation is very interesting astrophysically: this is how binary white dwarfs formed in wide stellar systems can be found.

Precision multicolor photometry provides a very adequate replacement of spectrophotometry as a means to address this problem. The "quasi-spectrum" resulting from multicolor photometry has very poor resolution, but each of its points has a low uncertainty.

[1] The General Catalog of Variable Stars team is currently revising their criteria for including new variable stars in the catalog [32].

[2] The General Catalog of Variable Stars contains more than 40 000 stars [31] and the AAVSO database about 180 000 variable stars [33].

3.8. Extragalactic Astronomy

Extragalactic astronomy is represented in the Lyra-B experiment through observations of galaxies. During the survey, galactic disks or bulges may be detected as extended objects, and their distinct star-like nuclei as point objects.

The observational techniques applied to extended parts of galaxies do not differ from those described in Section 3.3.4. The typical central brightness of the bulge in a moderate-luminosity spiral galaxy is about $18^m/(\text{arcsec})^2$. The surface brightnesses of galactic disks are lower, within $21^m/(\text{arcsec})^2$. Both these values refer to the B band. Since the B-band detection threshold for the Lyra-B survey is 20.3^m (see Section 6), galaxies with bulges will be detected and those possessing no bulges will not. Since an object's surface brightness does not depend on its distance, we will be able to detect all galaxies whose bulges have angular sizes exceeding two to three pixels; i.e., $1.5''-2''$. The mean effective radius of a typical bulge is about 0.8 kpc [34]; thus, the bulges will be larger than $1.5''-2''$ for galaxies that are closer than 80 Mpc. Since about 40% of galaxies possess bulges, the expected number of galaxies to be detected as extended objects in the Lyra-B experiment is several tens of thousands.

Independent of the "bodies" of galaxies, compact, star-like galactic nuclei will be detected. The detection threshold for these nuclei is the same as for stars: 16^m and 17^m in the V and B bands. Hubble Space Telescope (HST) observations have demonstrated the typical absolute magnitudes of star-like nuclei in spiral galaxies to be $-14^m < M_B < -10^m$ [35], and in dwarf elliptical galaxies to be $-13^m < M_B < -11^m$ [36]. Thus, star-like nuclei of these brightnesses can be detected in dwarf galaxies at distances not exceeding 10 Mpc, and in moderate-luminosity spiral galaxies at distances not exceeding 16 Mpc, which corresponds to the distance to the Virgo cluster. The statistics HST show that distinct nuclei are observed for about 75% of late-type spiral galaxies [37] and about 55% of disk galaxies, over the entire range of morphological types [35]. Applying these numbers to the catalog of galaxies in the local Universe [38], suggests that we can expect the Lyra-B experiment to detect about 100 star-like galactic nuclei.

3.9. Astrometry

The diameters of point-source images formed with the Lyra-B telescope are approximately 1.5 pixels over the entire focal plane. This value is nearly optimal for determining the coordinates for point sources. The uncertainty in the position of the center of brightness in such an image depends, first and foremost, on the signal-to-noise ratio. The center of brightness can be determined for bright stars with accuracy to 0.01 pixels or better. However, vibrations of the ISS will interfere with high-precision astrometric measurements, and deteriorate the expected accuracy of measurements of stellar coordinates. Our estimates show that, despite this problem, the uncertainties of astrometric measurements will be of the order of 1 mas for all stars detected in the survey; the uncertainty in the coordinates for stars brighter than 12^m will not exceed 100 microarcseconds. For faint stars, this is comparable to the Hipparcos results, while the Lyra-B uncertainty is somewhat higher for bright stars. Measurements with the Lyra-B telescope will make it possible to measure parallaxes of stars at distances to 1 kpc or somewhat more with uncertainties of 10%.

Note that here we are referring to measurements of the relative positions of objects. Such uncertainties will be achieved for objects that can be simultaneously detected in the focal plane of the telescope, i.e., at distances from each other not exceeding 1°. The Lyra-B project is not planning to derive a fundamental coordinate system.

3.10. Gaia and Lyra-B

The launch of the large astrometric satellite Gaia developed by the European Space Agency [29] is scheduled for 2013. It will measure stellar coordinates in the optical with unprecedented accuracy: to ~25 mas for 10^m stars and 0.3–1.0 mas for 20^m stars. It will also perform multicolor "quasi-photometry" of the measured stars and determine their radial velocities. If the design of the Gaia satellite had remained the same as in the draft project description [39], there would have been no need for the Lyra-B experiment. The initial version included the ability to carry out classical multicolor photometry with special light detectors for each band, etc. However, the current design is considerably more limited: the ability to carry out photometry was replaced with low-resolution spectroscopy,[3] with subsequent computation of the fluxes in spectral bands [29]. This naturally degraded the photometric accuracy to the level of typical ground-based uncertainties of $0.02^m-0.03^m$.

Merging the astrometric part of the Gaia catalog with the Lyra-B photometric catalog will create a super-catalog with fundamentally new information. Note also that the catalogs will be created virtually

[3] Thirty-four and 36 bins in the red and blue, respectively.

simultaneously,[4] and that the best measurement accuracies for the two experiments will be achieved for the same stars, i.e., those brighter than 12^m.

4. PRINCIPLES OF THE LYRA-B EXPERIMENT

The ISS orbits the Earth maintaining its so-called "orbital orientation" [27], with the ISS always turning the same ("bottom") side toward the Earth. Instruments for observations of the Earth are located on this side. The opposite side, directed toward the local zenith, is for instruments observing outer space.

In its orbital orientation, the station's longitudinal axis is directed approximately along its orbital velocity vector. The Russian segment of the ISS is in its "tail."

4.1. Techniques for Observations of the Celestial Sphere

Two techniques can be used to perform observations from the ISS: (1) a direct-pointing mode and (2) a scanning mode. Most ground-based telescopes and space observatories operate in a direct-pointing mode. A scanning mode was used in the Hipparcos experiment [15] and the SDSS survey [14], and will be applied in the future JMAPS, JASMINE, and Gaia missions [29, 40, 41].

It is much easier to realize scanning observations than direct-pointing observations at the ISS. For this purpose, it is sufficient to put the telescope's optical system in a fixed position relative to the body of the station.[5] The telescope will rotate with the station as the ISS orbits the Earth, and stellar images will move into the focal plane of the telescope. It will be necessary to change the telescope's position only rarely, approximately once a month (see Section 6.6.1), increasing the reliability of the design.

The light detectors most often used in telescopes for photometry are either CCD chips or CMOS sensors and mosaics of these devices [42, 43]. During scanning observations, light detectors must be operated in a so-called time delay integration (TDI) mode[6] [44].

In the TDI mode, charges accumulated during the exposure time move along the chip at the same rate and in the same direction as the stars. This imposes requirements on the position of a CCD chip in the focal plane and the accuracy of setting the rate of motion of the charge.

The accumulated charge is read out when the image reaches the edge of the CCD chip. The resulting frame looks like a strip whose width is equal to the number of pixels in a single line of the CCD chip and whose length is determined by the duration of the observation and the rate of motion of the stars in the focal plane.

The TDI mode has a number of advantages that are important for high-precision photometry: it averages non-uniformities of sensitivity and thermal generation along the CCD columns, and provides stable thermal and electric conditions for the operation of the chip. The TDI mode also naturally provides a so-called "dithering mode" [45], which considerably reduces the thermal generation of electrons.

When performing multicolor photometry, several CCD chips lie in the focal plane, each with its own optical filter. These provide observations in the different spectral bands of the photometric system. In the scanning mode, the image of an object passes through all the CCD chips one after another, yielding quasi-simultaneous multicolor brightness measurements. The design of the light detector resembles that used in the telescopes used for the SDSS project [46].

4.2. The Telescope

The parameters of the telescope used in the Lyra-B experiment are dictated by the aims of the experiment and the limitations imposed by the ISS.

The size of the instrument is determined by the method for its delivery to and assembly at the ISS. Scientific equipment is delivered to the ISS using a "Progress" freight spacecraft, which is placed in a near-Earth orbit and then docked to the station. The delivered blocks of scientific equipment are then taken inside the Russian ISS segment trough internal hatches. Further, some of these blocks are taken outside and attached to the station's external surface. The strongest constraints on the telescope size are imposed by the parameters of the hatches and the process of moving cargo sections from the "Progress" spacecraft into the ISS. The largest possible diameter and length of a cargo section are 0.6 m and 1.3 m. Thus, taking into account the thickness of the telescope walls and transportation packing, the diameter of the primary mirror cannot exceed 0.5 m. Outside the ISS, the telescope will be assembled from three sections: (1) the main section, consisting of the telescope itself, its focal plane with the light detectors, and the electronic blocks; (2) the objective hood with a cover; and (3) a positioning device, used to attach the telescope to the ISS surface and to change its pointing. Since the crew onboard the ISS do not have

[4] The Gaia catalog starting in 2013 and the Lyra-B catalog starting in 2015.

[5] The issue of correcting for vibrations of the ISS is addressed in Section 5.

[6] This mode can be realized only for CCD chips, not for standard CMOS sensors.

the ability to assemble or align the optical system, the telescope must be brought to the ISS already assembled.

The size of the telescope's field of view is determined by several factors. An instrument with a fairly wide field of view is needed for the all-sky survey. On the other hand, the larger the field of view, the more difficult it becomes to satisfy the requirements for aberration of the telescope's optical system [47, 48]. At the same time, making and adjusting the optics becomes more complicated and expensive. Thus, we chose a compromise size for the corrected field of view $2\omega = 2°$. In this case, the angular size (diagonal) of the focal plane is 1.5° and the width of the scan strip is $W = 1°$. The rest of the corrected field of view is used for the light detectors of the image stabilization device (see Section 5).

The limiting angular resolution of the Lyra-B telescope should be not worse than $1''$. This is one of the main points of the experiment's requirement specifications. Using CCD chips with the technologically optimal pixel size, 12 μm×12 μm, we find the minimal focal length to be $F \approx 3$ m. In this case, the length of the telescope, together with the focal plane (without the hood), must not exceed 1.3 m to make it possible to move the telescope inside the ISS.

The telescope must also satisfy several other requirements. Since the light detectors are CCD chips, the instrument must have a flat image field.

Further, the full-width at half-intensity diameter of the image of a point source should be about 1.5–2 pixels over the entire focal plane. This requirement follows from the need to precisely determine the brightness and position of the centers of brightness of the images.

Finally, since the telescope operates in the scanning mode, it must satisfy fairly strong requirements regarding relative distortion (<0.1%). Otherwise, stellar images in the focal plane will deviate from the chip columns and become blurred.

The currently widely used Ritchey–Chrétien optical scheme with an afocal lens corrector satisfies all these requirements, and this scheme was selected for the telescope. The characteristics of the Lyra-B telescope are described in more detail in [49].

It is proposed to use silicon carbide for the telescope mirrors. There are two reasons for this choice [50]. First, silicon carbide is very rigid, making it possible to construct thin and light mirrors that satisfy the mass constraints of the design. Second, silicon carbide has a very high thermal conductivity, so that mirrors made of this material exhibit only small non-linear distortions of their shapes and quickly reach thermal equilibrium.

4.3. Observational Coverage of the Celestial Sphere

In the Lyra-B experiment, the principle orientation of the telescope is such that its optical axis is in the orbital plane of the ISS. In this case, the center of the instrument's field of view moves along a great circle whose plane coincides with the orbital plane of the station. The ISS orbit is inclined to the Earth's equator by approximately 51.6° (this inclination does not change in time by more than 0.1°). The ISS orbit precesses with a period of about 70 days due to perturbation by the Earth's gravitation field [27]. This precession rate corresponds to a displacement of the instrument's field of view along the equator by 0.3° per orbit; i.e., each object enters the 1°-wide scanning strip of the telescope at least four times during a series of successive orbits.

Due to precession, the telescope field of view covers a spherical belt of the sky with coordinates $|\delta| < 52.1°$. (The width of this belt is twice the ISS orbital inclination, $2 \times 51.6°$, plus the width of the scanning strip, 1.0°.) Regions near the celestial poles remain unobserved (Fig. 1a). To make the scanning strip pass through the North celestial pole, it is necessary to move the telescope axis North of the orbital plane by 38.4° (Fig. 1b). Scanning the South pole requires the same change in orientation toward the South.

The entire sky can be covered with observations by combining these three modes. To make the scanning of the celestial sphere more effective, it may also be necessary to implement additional intermediate orientations of the telescope. Note that orientations of the telescope axis deviating from the ISS orbital plane by more than 38.4° should not be used, since they drastically increase problems related to the curvature of the trajectories along which stellar images move in the focal plane.

Observations are possible only for the portion of the orbit where illumination by scattered solar light is absent or low. Observations of objects close to the limiting magnitude are optimized when the ISS is in the shadow of the Earth. For the part of the orbit illuminated by the Sun, the minimum angle between the instrument's optical axis and the direction toward the Sun is determined by the effectiveness of the hood. It is currently possible to guarantee that the hood will attenuate scattered light by a factor of 10^6. This means that it will be possible to observe limiting-magnitude objects in the absence of direct illumination of the telescope's entrance aperture; i.e., when the angle between the axis of the telescope and the edge of the solar disk is greater than 90°. Only the brightest objects are observable for the rest of the orbit.

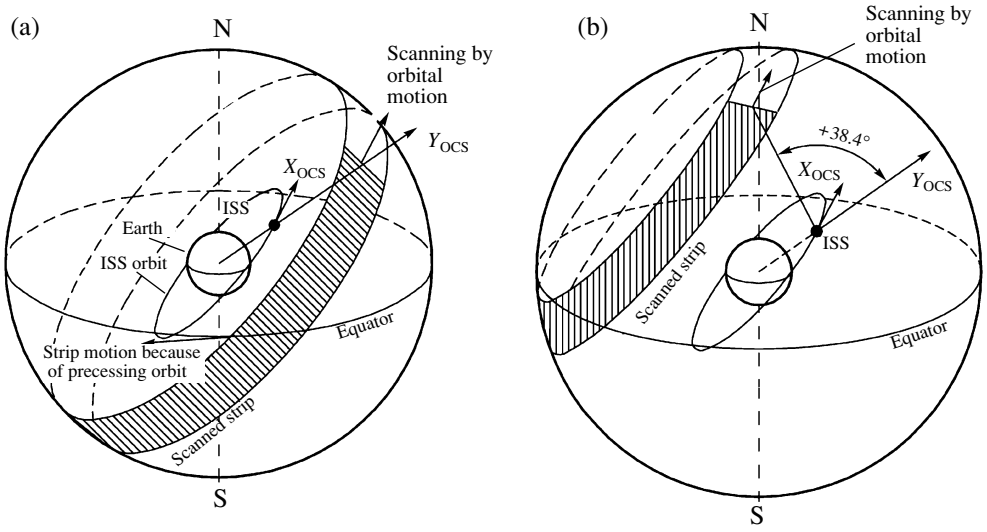

Fig. 1. Scanning the sky. (a) Scanning in the case of the principal orientation of the instrument; i.e., with the telescope axis in the orbital plane. (b) The telescope axis is moved 38.4° to the North, and the scanned strip covers the North celestial pole.

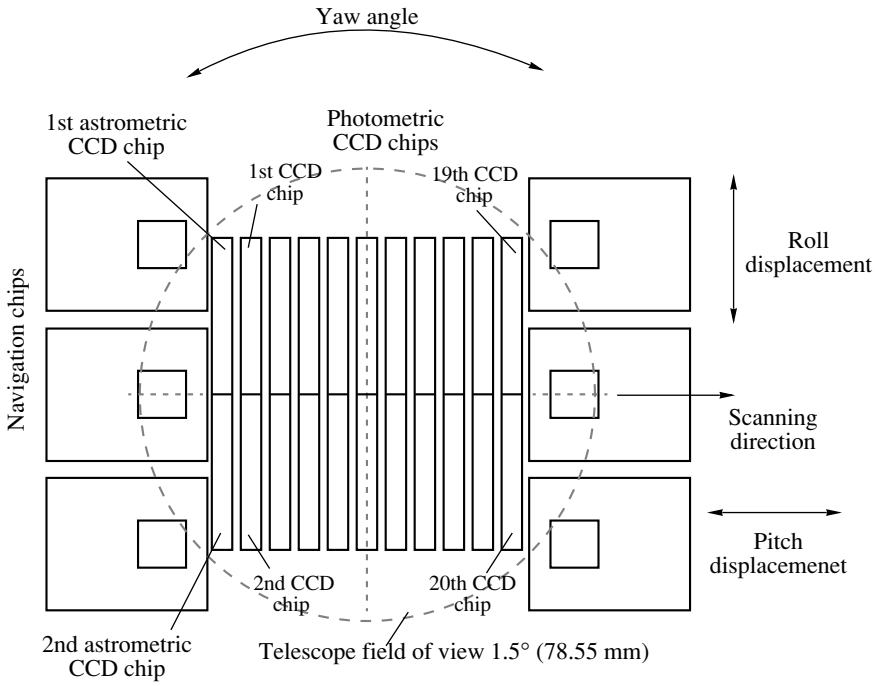

Fig. 2. Design of the focal plane in the Lyra-B experiment.

4.4. Light Detectors and Photometric System

An assembly of 11 back-illuminated CCD chips is proposed as the photometric light detector. The design of the assembly is shown in Fig. 2. Each chip consists of two parts, 2250 × 300 pixels in size, which operate independently.

The firm "e2v Technologies Ltd" (UK) has indicated its ability to make such CCD chips especially for the Lyra-B space experiment. Some technical parameters of these chips are collected in Table 2.

The first CCD[7] will be covered with a broadband, transparent (panchromatic) coating, and the other chips with interference optical filters realizing the Lyra-B photometric system. The filter passbands of the photometric system are presented in Fig. 3 and

[7] The CCDs are numbered in the direction of motion of stellar images.

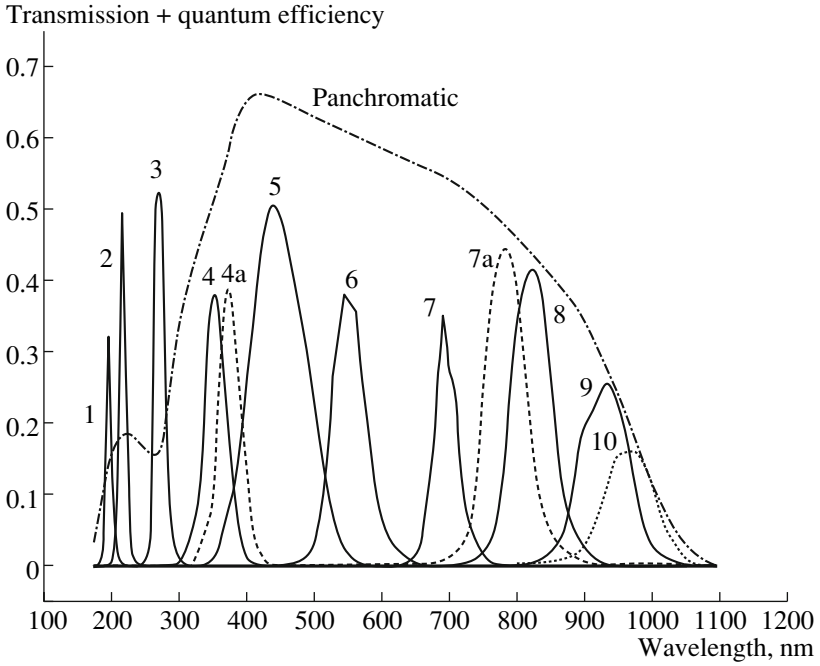

Fig. 3. The passbands of the Lyra-B photometric system, with the central wavelengths 195 nm (1), 218 nm (2), 270 nm (3), 350 nm (4), 374 nm (4a), 440 nm (5), 555 nm (6), 700 nm (7), 785 nm (7a), 825 nm (8), 930 nm (9), 1000 nm (10), and the broadband panchromatic filter. The passbands take into account the transmission of the interference filter covering the silicon and the CCD quantum efficiency.

Table 3. This figure and table present 12 photometric bands, while there will be only 10 detectors; i.e., two of the listed filters will be excluded.

All bands of the Lyra-B photometric system are in the sensitivity range of ordinary silicon back-illuminated CCD chips. The first three UV filters—195, 218, and 270 nm—can be used to study hot stars and to efficiently determine interstellar extinctions; the 218 nm filter is in the center of an UV interstellar extinction band and the two other filters on either side of this band. The four bands at 350, 440, 555, and 700 nm are close to the W, B, V, and R bands of the modified Johnson–Cousins system. These four bands were used in the SAI's Tian Shan $WBVR$ catalog [16, 51].

The 374 nm filter is at the Balmer jump, and can serve for identification of blue and white supergiants. This also coincides with the P band of the Vilnius photometric system [52], but is wider. The remaining bands are in the near-IR. The 785 nm filter is at a local minimum between two TiO bands, and the 700 and 825 nm filters are at local maxima in the spectra of M stars. The 930 nm filter corresponds to an atmospheric water band, and will serve for determining atmospheric parameters during follow-up ground-based observations of stars from the catalog. The 1000 nm filter covers the longest-wavelength part of the sensitivity range of silicon CCDs.

Although the suggested photometric system is broadband, it will enable fairly high-quality three-dimensional classification of stars. Further changes in the photometric-band parameters are still possible. For a more detailed explanation of this choice of bands for the Lyra-B photometric system, see [28, 53].

Table 2. Characteristics of the photometric CCDs proposed by e2v Technologies Ltd

Chip size	4500 × 312 pixels*
Pixel size	12μm×12 μm
Pixel capacity	200 000 electrons
CCD thickness for the visual	14 μm
CCD thickness for the IR	30 μm
Maximum quantum efficiency of the panchromatic CCD	96%
Readout noise at 1 MHz	5 electrons per pixel
The same, for differential readout	7 electrons per pixel
Thermally generated noise at $T = -30°$C	<1 electrons pixel^{-1}s^{-1}

* A CCD consists of two independently operated sections, each 2250 × 312 pixels in size.

It is proposed to place the interference filters directly as coatings on the CCD chips. This technology was developed in the Physical Institute of Russian Academy of Sciences [54], and was successfully tested in experiments onboard spacecraft of the Coronas series. This technique can be used only for back-illuminated chips with smooth, uniform front surfaces.

An interference optical filter is usually formed by a glass plate with an interference coating placed in front of the light detector. Reflections from both surfaces of the glass plate and from the front surface of the CCD chip create numerous regions of glare, especially for bright stars. The technique of filter coating described above makes it possible to avoid these effects.

4.5. Detection of Objects

The Lyra-B experiment does not use an input catalog for photometry of point objects (stars and compact galaxies). There is only an input catalog of extended objects (nebulae, clusters, and nearby galaxies) for surface photometry and a catalog of the brightest stars that will overflow the CCD pixels.

Point objects will be measured in the following way.

1. The image created by the first chip with its panchromatic coating, which has the highest sensitivity, will be read out fully. A search will then be performed in the resulting image for objects significantly exceeding the noise level (with signal-to-noise ratios >10). The coordinates, brightnesses, and other parameters will be determined for identified objects. These will then be used to pre-calculate the positions and arrival times for all other photometric chips in the focal plane for each detected object. The list of detected point objects will be added to the list of extended objects from the corresponding input catalog. The arrival times and positions in the other chips will also be calculated for them.

2. A full readout will be performed for the pre-calculated fragments of the other chips. The size adopted for point sources will be constant and equal to 7×7 pixels (this value may be revised in the future). The fragments for very bright stars that saturate image pixels and for extended objects can be larger and have a rectangular shape.

Signals in the intervals between the boundaries of fragments containing images of objects will be summed without readout along parts of the CCD-chip rows up to 100–150 pixels in length (i.e., in fields up to $1 \times (100–150)$ pixels in size). The signal in the intervals between objects is due to background stars and unresolved objects. This amounts to several photons per pixel during the exposure time. These regions will be summed without readout so that the readout noise will be introduced into the measured signal only once.

3. Images in the most sensitive bands of the photometric system (V, B, and R) can be used to determine the instantaneous positions of an object's center of brightness and find its displacement and blurring during the passage across the focal plane. This procedure will make it possible to identify solar-system objects moving sufficiently rapidly on the celestial sphere in real time.

Table 3. Passband parameters for the Lyra-B photometric system (central wavelengths, photometric passband widths, optical-filter maximum transparencies, overall sensitivities of light detectors at maximum)

λ_0, nm	$\Delta\lambda$, nm	Fil, %	Fil + QE, %
195	20	73	32
218	20	84	49
270	25	82	52
350	50	59	38
374	50	59	38
440	100	73	50
550	80	55	37
700	80	53	35
785	80	74	41
825	80	74	41
930	80	72	25
1000	100	76	16
Panchromatic*	∼600	91	66

* The transmission maximum of the panchromatic filter is at $\lambda = 495$ nm and the sensitivity maximum of the panchromatic detector of light is at $\lambda = 415$ nm.

4.6. Observations of the Brightest Stars

The capacity of a CCD pixel is limited, and depends primarily on its linear size [42]. The CCD chips manufactured by the e2v technologies ltd., which are planned for use in the Lyra-B experiments, have a pixel size of 12 μm $\times$ 12 μm and a capacity of 200 000 electrons. If the signal is higher, the accumulated electrons will flow into the potential wells of adjacent pixels, back and forth along a column. Since the brightest part of a stellar image occupies 2×2 pixels (see Section 4.4.2), the largest accumulated charge will be about 800 000 electrons. Taking into account the detector noise, a significant signal begins

to be registered for approximately 200 electrons. This means that it is possible to simultaneously measure objects that give numbers of accumulated electrons from 200 to 800 000. The brightness of such objects differs by no more than 8^m.

Accurate photometry of brighter stars simultaneous with fainter ones becomes impossible.

Therefore, photometry of the brightest stars will be performed in a special mode, in which it is necessary to distribute the accumulated signal among a large number of pixels. The simplest way to do this is to defocus the image. Defocused images move the dynamic range of the light detectors towards higher fluxes. The faintest stars, which are close to the survey limit, will not be detectable in this mode, but bright and the brightest stars will be observable instead.

The brightest stars can be observed in the presence of stronger solar illumination; i.e., with smaller angles between the telescope axis and the direction toward the Sun. This mode can be scheduled for the beginning and end of each observing session (at the beginning and towards the end of each scan of the sky).

4.7. Calibration of the Light Detectors

The sensitivity of the CCD chips and the transmission curves of the filters covering them will change with time. The main factors causing these variations are the influence of the ISS microatmosphere and energetic particles [55]. These factors must be taken into account in order to achieve stable photometric results, since the Lyra-B experiment will continue over several years.

It was decided to regularly perform calibration procedures to determine the characteristics of the photometric equipment. We plan to use three types of calibration.

1. Calibration using sunlight. For this procedure, the light detector is illuminated with scattered sunlight.

2. Calibration using internal sources of light. It is planned to install several light sources inside the telescope: UV and broadband ("white") light-emitting diodes (LEDs). A narrowband acoustic–optical filter [56, 57] that transmits light in a band several nanometers wide with the central wavelength varying between 400 and 800 nm will be installed in front of one group of white LEDs. This device can be used to check the light-sensitivity curves of the CCDs.

3. Comparison with ground-based observations. Another way to study the deterioration of the light detectors in the Lyra-B experiment is to perform ground-based observations of stars using light detectors similar to those onboard the ISS that have been calibrated under laboratory conditions.

5. REASONS FOR PERFORMING THE EXPERIMENT ONBOARD THE ISS AND PROBLEMS DUE TO THIS CONFIGURATION

The choice of the ISS as the site of the Lyra-B experiment has both advantages and disadvantages. An alternative would be to launch a free-flying satellite.

We consider the following to be substantial advantages of using the ISS as the site of the experiment:

- the existence of technological and technical infrastructure: energy sources, information channels, the possibility of obtaining information on the station's position, etc.;
- tested technology for the delivery of low- and moderate-weight equipment onboard;
- the possibility of returning the payload to the Earth (with strong weight limitations);
- assembly of the equipment by the station crew;
- the possibility of repairing the equipment, if urgently needed, by the station crew.

However, the main reason to choose the ISS as the site of the Lyra-B experiment is the large volume of scientific data that must be transmitted to the Earth. The data flow during observing sessions is about 300 Mbits per second. The complete volume of data that will be accumulated during the experiment and must be transmitted to the Earth is about 200 Tbytes.

Standard means of space radio communications have insufficient speeds for transmitting information, of the order of several Mbits per second. In addition, continuous transmission of information requires that the spacecraft remain in direct visibility of the ground-base receiving station at least during the entire observing session. Since the number of receiving antennas is limited, this is possible only for geostationary (geosynchronous) or highly elliptical orbits.

The ISS also does not possess a communication channel that would enable transmission of the accumulated information flow. Thus, we have chosen a different way to transmit the data to the Earth: the data from the telescope will be sent to the control unit for the scientific experiment, installed in a hermetic compartment of the ISS. There the data will be written on removable external recording media, which will then be sent to the Earth with the returned payload (twice

a year). The proposed recording media are assemblies of flash memory units. These devices are very reliable and are among those with the currently best ratio of recorded information to mass, about 10 Tbytes per kilogram.

This approach is able to pass the full volume of scientific information, but is completely lacking in promptness. Fortunately, the survey character of the experiment makes promptness of the information transfer unimportant for most scientific problems to be studied (see Section 3).

Placing the scientific equipment onboard the ISS also has a number of disadvantages. One of the drawbacks that is most serious for observations in the visible using telescopes with angular resolutions better than one arcsecond are vibrations of the manned station due to the activity of the crew and the operation of the life-supporting systems. This is why manned stations have not been used so far for astronomical observations requiring one-second accuracy of the angular stability of the equipment.

This problem also exists for the Lyra-B experiment.[8] To overcome this, a special image-stabilizing system, to be built into the telescope, has been designed. Shifts will be compensated for by moving the focal plane with a high-accuracy piezo-mechanical hexapod (a Gough–Stewart platform) [58], which is a kind of modern, automated version of the Ritchey plateholder [59, Section 6].

6. EXPECTED SURVEY RESULTS AND STRUCTURE OF RESULTING SCIENTIFIC DATA

6.1. Number of Observations per Object

We modeled the situation in order to estimate the coverage of the celestial sphere that will be obtained. A scanning schedule was worked out for an arbitrarily chosen one-year interval. Observations were assumed possible when the ISS was in the Earth's shadow and, outside the shadow, if the angle between the telescope axis and the solar limb exceeded 90°. Of the three basic orientations of the telescope (in the orbital plane and the Southern and Northern polar orientations; Section 4.4.3), we chose the orientation that would enable the longest observing sessions, taking into account the illumination. The telescope orientation is changed 14 times in a typical observing schedule. The model observations were carried out over 193.4 days (53% of the observing time); scanning in the orbital plane took 52.2 days and scanning of the polar regions 70.6 days each. The mean number of observations[9] for an individual object was 22 per year, and reached 1000 for objects near the celestial poles. Our model did not take into account gaps in the observations during docking and crew activities outside the station, which are expected to reduce the observing time by approximately 10%.

Based on the above modeling, the mean number of observations of an individual object will be 100 over the five years of the experiment.

Table 4. Limiting magnitudes of the Lyra-B A0V-star survey

λ_0, nm	Limiting magnitudes				CCD overflow
	One observation		In five years*		
	0.01^m (1%)	0.1^m (10%)	0.01^m (1%)	0.1^m (10%)	
	S/N				
	100	10	100	10	
195	8.5	13.2	13.2	16.3	3.6
218	9.0	13.6	13.6	16.8	4.2
270	9.4	14.1	14.1	17.3	5.4
350	10.6	15.3	15.3	18.4	6.5
374	10.7	15.4	15.4	18.6	7.1
440	12.6	17.3	17.3	20.4	8.5
550	11.6	16.3	16.3	19.5	7.4
700	11.1	15.8	15.8	18.9	6.0
785	11.0	15.7	15.7	18.7	7.4
825	10.8	15.5	15.5	18.5	7.2
930	10.3	14.9	14.9	18.0	6.8
1000	9.7	14.3	14.3	17.4	6.3
Panchromatic	14.0	18.5	18.5	21.4	10.3

* The S/N values for 0.1^m for one observation and 0.01^m in five years are the same, because we assumed the mean number of observations of a star over five years to be 100. The S/N values for 0.1^m in five years correspond to averaging 100 observations for stars detected in single observations with $S/N = 10$. This situation is valid for observations of regions recorded pixel-by-pixel.

6.2. Limiting Magnitudes

The pixel size of our photometric CCDs is 12 μm, which corresponds to an angular size of 0.8″ for the

[8] The ISS was designed, among other things, for experiments occurring under microgravity conditions, so its vibrations are weaker than those of earlier manned stations, such as the "Mir" station.

[9] An individual observation corresponds to a single passage of an object across the focal plane; i.e., measurements in the panchromatic filter and in the ten bands of the photometric system.

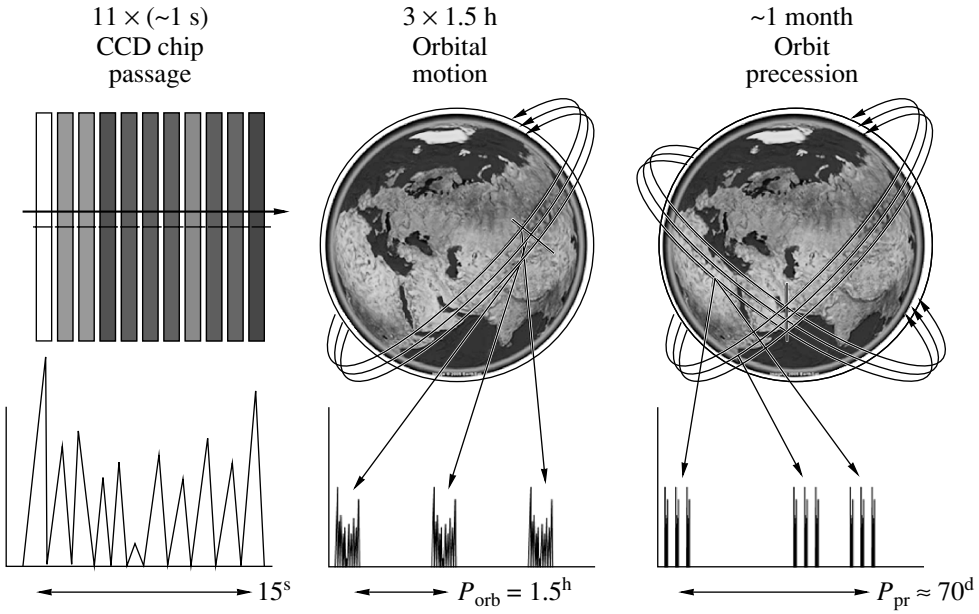

Fig. 4. Time scales represented in observations during the Lyra-B space experiment.

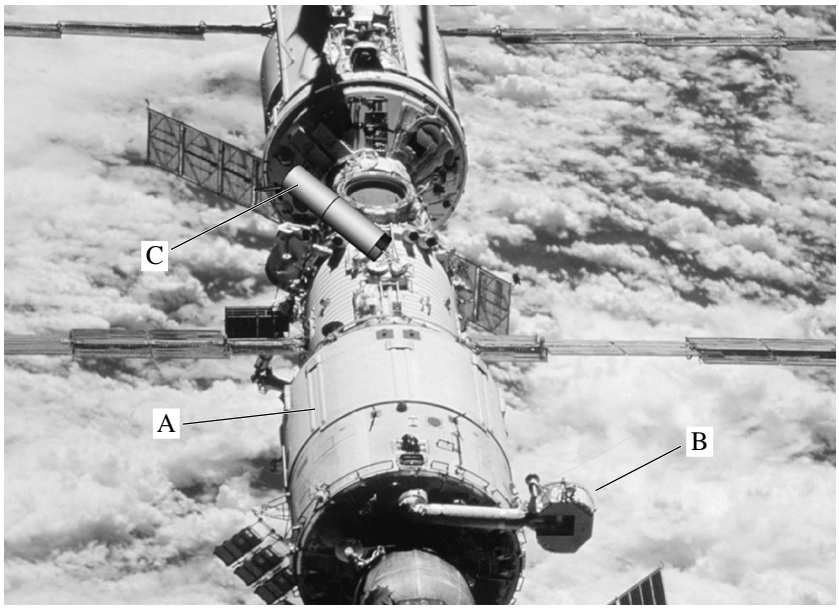

Fig. 5. The Russian ISS segment, with the "Zvezda" service module (A), narrow-beam Lyra antenna (B), and Lyra-B telescope (C) marked.

telescope focal length, $F = 3$ m. Since the ISS makes one orbit in 1.5 h, the exposure time, understood as the time needed to cross one CCD (along the side that is 300 pixels long) when scanning the sky in the ISS orbital plane is $\tau = 1.04$ s. The derived exposure time, along with the above parameters of the telescope and filters, can be used to calculate the limiting magnitudes for each spectral band. These data are presented in Table 4.

The columns of Table 4 contain (1) the central wavelengths of the photometric bands, (2), (3) the limiting magnitudes of objects with single-measurement uncertainties of 0.01^m (1%) and 0.1^m (10%), (4), (5) the limiting magnitudes of non-variable objects whose measurement uncertainties averaged over all observations during the experiment (100 observations in five years) are 0.01^m (1%) and 0.1^m (10%), and (6) the magnitudes of point

Table 5. Limiting V magnitudes of the Lyra-B survey of A, F, G, and K stars

λ_0, nm	One observation, 0.01^m				One observation, 0.1^m			
	A	F	G	K	A	F	G	K
195	8.5	6.1	1.6	−0.6	13.2	10.8	6.3	4.1
218	9.0	7.3	4.3	0.0	13.6	12.0	9.0	4.6
270	9.4	8.4	7.2	5.0	14.1	13.1	11.8	9.7
350	10.6	10.3	9.8	8.9	15.3	15.0	14.5	13.6
374	10.7	10.4	9.8	9.0	15.4	15.1	14.5	13.7
440	12.6	12.5	12.3	12.1	17.3	17.1	16.9	16.8
550	11.6	11.8	11.9	12.1	16.3	16.4	16.6	16.8
700	11.1	11.5	11.9	12.4	15.8	16.2	16.6	17.1
785	11.0	11.5	12.0	12.6	15.7	16.1	16.6	17.2
825	10.8	11.3	11.8	12.5	15.5	16.0	16.5	17.1
930	10.3	10.8	11.3	12.0	14.9	15.4	16.0	16.7
1000	9.7	10.2	10.8	11.5	14.3	14.9	15.4	16.2
Panchromatic	14.0	14.1	14.2	14.5	18.5	18.6	18.7	19.1

objects bright enough to yield an overflow of CCD pixel capacity during a single measurement. The magnitudes in the table were estimated for A0V stars.

Table 5 presents the limiting magnitudes for stars of several spectral types. These results were taken from [26], where the assumptions made to obtain these values are described in detail. Note that Table 5 contains limiting magnitudes for stars in the V band rather than the spectral band planned for the observations.

6.3. Time Structure of the Observations

Three different time scales are present in observations of objects during the Lyra-B experiment.

The shortest time scale is related to the sequential passages of an object's image across the 11 CCD chips in the focal plane. The interval between passages through adjacent chips is about 1 s.

An intermediate time scale is related to observations of an object made during two sequential orbits, which are separated by about 1.5 h. Objects are observed on four (or more) sequential orbits.

The longest time scale is related to the successive appearances of an object in a scanned strip. Such appearances do not occur strictly periodically, because an object cannot be observed when it is close to the Sun; at other times, the observing schedule depends on the schedule for changing the telescope orientation. This time scale is typically about a month.

These time scales are shown schematically in Fig. 4.

7. CONCLUSIONS

Our active work on the Lyra-B project started toward the end of 2007. We prepared a preliminary design in 2008, and a draft design for the Lyra-B space experiment itself in 2009–2010. The scientific part of the Lyra-B experiment is coordinated by the SAI; the main producer of the scientific equipment for the project is the Saint-Petersburg National Research University of Information Technologies, Mechanics and Optics. At these stages, we demonstrated the possibility of carrying out the experiment and achieving the characteristics indicated in its specification, the most important of which were described earlier this paper.

If the time schedule proposed at the completion of the draft design can be adhered to, the realization of the Lyra-B experiment can begin towards the end of 2015.

ACKNOWLEDGMENTS

The authors wish to thank O.K. Sil'chenko and A.S. Rastorguev for helpful discussions of the scientific program of the Lyra-B experiment. We are especially grateful to A.M. Cherepashchuk for his invaluable assistance during initial formulation of the project and his extensive further support.

APPENDIX

THE NAME OF THE "LYRA-B" PROJECT

The Lyra-B project was included in a long-term space research program in 1999. Since then, the developers of the program have repeatedly been asked about its name, most often through two questions: «Why "Lyra"?» and «"Where did "B" come from?».

From the beginning, this was planned as a photometric project. The main reference object for all stellar photometric systems is Vega. However, it was not possible to name the space mission "Vega", since this was the name of two space probes sent to comet Halley in 1984–1986 [60], although these probes were named, not after the star, but as an abbreviation of the Russian words for Venus and Halley.

Vega is the brightest star (α) in the constellation of Lyra, and the name used for the International Space Station, at that time, was "Alpha Station." Because of this coincidence, the name of the constellation was adopted as the main name for the experiments proposed by the SAI.

Both names—"Vega" and "Lyra"—were suggested by A.M. Cherepashchuk, the director of the SAI.

The letter "B" appeared in the name of the project twice. First, at the initial proposal stage, two projects were put forward. The first was a telescope with super-smooth mirrors forming an out-of-eclipse mirror coronograph. After super-polishing, these silicon mirrors should have had a surface error of the order of 1/100 of a wavelength, making it possible to observe faint galaxies around quasars and planets (brown dwarfs) near stars. This project was called Lyra-A.

The second project was aimed at a whole-sky photometric survey, and was a simpler version of the experiment described in the present paper. This received the name Lyra-B.

It soon became clear that the stellar environments of quasars and exoplanets were too faint for telescopes with a maximum diameter of 0.5 m and a longest exposure time of about 45 min, such as it is possible to assemble and use onboard the ISS. As the result, the Lyra-A project was cancelled; there remained only the photometric survey Lyra-B, and the letter "B" was removed from its name.

Thus, when the proposal for this experiment was included in the long-term space research program, the project had the name Lyra, without any additional letter. However, it soon became known that there already existed a device among the equipment onboard the Russian ISS segment called "Lyra." This is an antenna installed in the "Zvezda" module and used for communications carried out with the Luch geostationary retranslation system [61] (Fig. 5). The operational capability of this system began to return in 2012, after the launch of the Luch-5A spacecraft.

According to regulations concerning the rules for naming space experiments onboard the ISS, all equipment and experiments must have unique names. For this reason, we added the letter "B" to the name of our experiment, so that Lyra-B returned.

REFERENCES

1. G. O. Abell, Astron. Soc. Pacif. Leaflets **8**, 121 (1959).
2. I. N. Reid, C. Brewer, R. J. Brucato, et al., Publ. Astron. Soc. Pacif. **103**, 661 (1991).
3. R. R. Gal, R. R. de Carvalho, S. C. Odewahn, et al., Astron. J. **128**, 3082 (2004).
4. B. M. Lasker, C. R. Sturch, B. J. McLean, et al., Astron. J. **99**, 2019 (1990).
5. B. M. Lasker, C. R. Sturch, B. J. McLean, et al., Astron. J. **99**, 2173 (1990).
6. J. L. Russel, B. M. Lasker, B. J. McLean, et al., Astron. J. **99**, 2059 (1990).
7. H. Jenkner, B. M. Lasker, C. R. Sturch, et al., Astron. J. **99**, 2082 (1990).
8. J. E. Morrison, S. Roeser, B. McLean, et al., Astron. J. **121**, 1752 (2001).
9. B. Lasker, M. G. Lattanzi, B. J. McLean, et al., Astron. J. **136**, 735 (2008).
10. E. Høg, C. Fabricius, V. V. Makarov, et al., Astron. Astrophys. **355**, L27 (2000).
11. D. Monet, *USNO-A V2.0* (U. S. Naval Observatory, Flagstaff, AZ, 1998).
12. D. G. Monet, S. E. Levine, B. Casian, et al., Astron. J. **125**, 984 (2003).
13. M. F. Skrutskie, R. M. Cutri, R. Stiening, et al., Astron. J. **131**, 1163 (2006).
14. J. K. Adelman-McCarthy, M. A. Agüeros, Allam, et al., Astrophys. J. Suppl. Ser. **172**, 634 (2007).
15. *The Hipparcos and Tycho Catalogues*, ESA SP-1200 (European Space Agency, 1997).
16. V. G. Kornilov, I. M. Volkov, A. I. Zakharov, et al., Tr. Gos. Astron. Inst. Shternberga **63**, 3 (1991).
17. A. V. Mironov, *Fundamentals of Astrophotometry: Practical. Basics of Stellar Photometry and Spectrophotometry* (Fizmatlit, Moscow, 2008) [in Russian].
18. A. Mironov and A. Zakharov, Astrophys. Space Sci. **280**, 71 (2002).
19. A. I. Zakharov, A. V. Mironov, and A. N. Krutyakov, Tr. Gos. Astron. Inst. Shternberga **70**, 289 (2004).
20. D. C. Martin, J. Fanson, D. Schiminovich, et al., Astrophys. J. Lett. **619**, L1 (2005).
21. W. Wamsteker, ASP Conf. Ser. **164**, 261 (1999).
22. N. Epchtein, B. de Batz, E. Copet, et al., Astrophys. Space Sci. **217**, 3 (1994).
23. E. L. Wright, P. R. M. Eisenhardt, A. K. Mainzer, et al., Astron. J. **140**, 1868 (2010).
24. V. Kornilov, Mon. Not. R. Astron. Soc. **417**, 1105 (2011).
25. V. G. Kornilov, Astron. Lett. **37**, 40 (2011).
26. A. V. Mironov et al., ASP Conf. Ser. (2012, in press).
27. N. Larter and A. Gonfalone, *International Space Station. A Guide for European Users*, Ed. by B. Battrick (Europ. Space Agency, Paris, 1996).

28. A. V. Mironov, A. V. Zakharov, and M. E. Prokhorov, in *Proceedings of the 37th International Student Conference on Space Physics* (Ural'sk. Gos. Univ., Ekaterinburg, 2008), p. 105.
29. M. A. C. Perryman, in *The Three-Dimensional Universe with Gaia*, Ed. by C. Turon, K. S. O'Flaherty, and M. A. C. Perryman, ESA SP-576 (European Space Agency, 2005), p. 15.
30. P. M. W. Kalberla and J. Kerp, Ann. Rev. Astron. Astrophys. **47**, 27 (2009).
31. N. N. Samus, O. V. Durlevich, E. V. Kazarovets, et al., *General Catalog of Variable Stars. GCVS Database*, vers. 2011Jan., CDS B/gcvs.
32. N. N. Samus, The Draft Classification for New GCVS Versions. http://www.sai.msu.su/gcvs/future/classif.htm.
33. C. L. Watson, in *The Society for Astronomical Sciences 25th Annual Symposium on Telescope Science*, Ed. by B. D. Warner, J. L. Foote, D. Mais, and D. Kenyon (Soc. Astron. Sci., 2006), p. 47.
34. A. W. Graham and C. C. Worley, Mon. Not. R. Astron. Soc. **388**, 1708 (2008).
35. S. Scarlata, M. Stiavelli, M. A. Hughes, et al., Astron. J. **128**, 1124 (2004).
36. S. Paudel, T. Lisker, and H. Kuntschner, Mon. Not. R. Astron. Soc. **413**, 1764 (2011).
37. T. Boeker, R. P. van der Marel, S. Laine, et al., Astron. J. **123**, 1389 (2002).
38. I. D. Karachentsev, V. E. Karachentseva, W. K. Huchtmeier, et al., Asron. J. **127**, 2031 (2004).
39. C. Jordi and E. Høg, in *The Three-Dimensional Universe with Gaia*, Ed. by C. Turon, K. S. O'Flaherty, and M. A. C. Perryman, ESA SP-576 (European Space Agency, 2005), p. 43.
40. B. N. Dorland, R. P. Dudik, Z. Dugan, et al., Bull. Am. Astron. Soc. **41**, 344 (2009).
41. N. Gouda, T. Tsujimoto, Y. Kobayashi, et al., Proc. SPIE **4850**, 1161 (2003).
42. S. B. Howell, *Handbook of CCD Astronomy* (Cambridge Univ. Press, Cambridge, 2006).
43. J. E. Beletic, J. W. Beletic, and P. Amico, *Scientific Detectors for Astronomy 2005*, Ed. by J. E. Beletic (Springer, Berlin, Dordrecht, 2006).
44. P. Martinez and A. Klotz, *A Practical Guide to CCD Astronomy* (Cambridge Univ. Press, Cambridge, 1998).
45. CCD Sensors Technical Note. Glossary of Terms. http://www.e2v.com/e2v/assets/File/documents/imaging-space-and-scientific-sensors/Papers/ccdtn106.pdf.
46. J. E. Gunn, M. Carr, C. Rockosi, et al., Astron. J. **116**, 3040 (1998).
47. G. M. Popov, *Modern Astronomical Optics* (Nauka, Moscow, 1988) [in Russian].
48. D. D. Maksutov, *Astronomical Optics* (Nauka, Moscow, 1979) [in Russian].
49. G.I. Zukanova, A.V. Bakholdin, J. Opt. Technol. **79**, 270 (2012)..
50. V. A. Alekseev, V. V. Bokov, V. N. Egorov, et al., Sov. J. Opt. Technol. **58**, 390 (1991).
51. Kh. Khaliullin, A. V. Mironov, and V. G. Moshkalyov, Astrophys. Space Sci. **111**, 291 (1985).
52. V. Straizhis, *Multicolor Stellar Photometry* (Mokslas, Vilnius [in Russian], 1977; Pachart, Tucson, 1992).
53. A. V. Mironov, A. I. Zakharov, M. E. Prokhorov, et al., in *Variable Stars, the Galactic Halo and Galaxy Formation,* Ed. by C. Sterken, N. Samus, and L. Szabados (Sternberg Astron. Inst, Moscow, 2010), p. 185.
54. TESIS: About Project. http://www.tesis.lebedev.ru/en/about_tesis.html.
55. K. D. Stefanov, T. Tsukamoto, A. Miyamoto, et al., Nucl. Instrum. Methods Phys. Res. A **436**, 182 (1999).
56. B. Bates, D. Findlay, and D. Halliwell, Proc. SPIE **369**, 315 (1983).
57. J. P. Xu and R. Stroud, *Acousto-Optic Devices: Principles, Design, and Applications* (Wiley, New York, 1992).
58. D. Stewart, Proc. Inst. Mech. Eng. **180** (15), 371 (1965).
59. D. Ya. Martynov, *Course of Practical Astrophysics* (Nauka, Moscow, 1977) [in Russian].
60. J. Blamont and R. Z. Sagdeev, Naturwissensch. **71**, 295 (1984).
61. *International Space Station. Communications.* http://en.wikipedia.org/wiki/International_Space_Station.

Translated by N. Samus'